

Transcranial magnetic stimulation induced fields in different brain models

M. Cvetković, D. Poljak, M. Rogić Vidaković & Z. Đogaš

To cite this article: M. Cvetković, D. Poljak, M. Rogić Vidaković & Z. Đogaš (2016): Transcranial magnetic stimulation induced fields in different brain models, Journal of Electromagnetic Waves and Applications, DOI: [10.1080/09205071.2016.1216807](https://doi.org/10.1080/09205071.2016.1216807)

To link to this article: <http://dx.doi.org/10.1080/09205071.2016.1216807>



Published online: 10 Aug 2016.



Submit your article to this journal [↗](#)



View related articles [↗](#)



View Crossmark data [↗](#)

Transcranial magnetic stimulation induced fields in different brain models

M. Cvetković^a, D. Poljak^a, M. Rogić Vidaković^b and Z. Đogaš^b

^aFaculty of Electrical Engineering, Mechanical Engineering and Naval Architecture, University of Split, Split, Croatia; ^bLaboratory for Human and Experimental Neurophysiology (LAHEN), Department of Neuroscience, School of Medicine, University of Split, Split, Croatia

ABSTRACT

This paper gives a comparison of the numerical results for the induced electric field, electric current density, and the magnetic flux density inside the adult, 10-years-old, and 5-years-old homogeneous brain models, for three different transcranial magnetic stimulation (TMS) coils. The numerical results are obtained using the TMS model based on the surface integral equation formulation and efficient numerical solution via Method of Moments. The two child brain models are obtained by linearly scaling the adult brain model. The age-dependent parameters of the brain are taken into account as well. The results show that the decrease in the homogeneous brain size results in the increased values of all TMS-induced fields. Implementing the age-related parameters significantly increases the induced current density values while moving the point with half maximum electric field value closer to the surface. The analysis undertaken in this work has underlined the importance of the brain size and the brain tissue conductivity in the modeling of TMS in children. Knowledge about the differences of the TMS-induced fields in adult and child brain models could potentially contribute to development of optimal TMS coils and stimulating parameters, which is especially important when applying TMS on pediatric patients in hospitals.

ARTICLE HISTORY

Received 7 March 2016
Accepted 18 July 2016

KEYWORDS

Transcranial magnetic stimulation; adult and child brain comparison; homogeneous human brain model; surface integral equation approach; electromagnetic model

1. Introduction

Transcranial magnetic stimulation (TMS) is a non-invasive and painless technique for stimulation or inhibition of certain brain areas. From the first demonstration more than 30 years ago, it has become very important in diagnostic and therapeutic purposes in the field of neurology, neurosurgery, neurophysiology, and psychiatry, as well as in studying functional mechanism and role of specific cortical regions.[1] Nowadays, navigated transcranial magnetic stimulation (nTMS) is becoming a standard technique in preoperative mapping of eloquent brain cortices (motor, speech, language) in patients undergoing awake brain surgery,[2,3] and in neurophysiologic development of nTMS methodologies for mapping these cortical areas in healthy subjects.[4,5]

Various clinical studies report different efficiency of TMS stimulation, primarily due to differences in relevant TMS settings such as coil positioning, pulse waveform, frequency,

number of stimuli, and the intensity of stimulation, to name only a few. Determination of optimal stimulation intensity is a problem many TMS studies are facing, specifically when mapping non-motor cortical areas. The single-pulse TMS mapping of the primary motor cortex has a well-established role in clinical neurophysiology. The generally accepted procedure is first to find the individual resting motor threshold (RMT) by stimulating the primary motor cortex for hand muscle and recording motor-evoked potentials (MEP) from hand muscle. RMT is defined as the minimum TMS intensity adequate to evoke MEPs in at least 50% of trials.[6] An extensive research has been carried out on the interindividual variability of the RMT [7,8] finding that the most important factor to this variability is the skull-to-cortex distance. Other neurophysiologic measures [9] include MEP amplitude and latency, cortical silent period duration, central motor conduction time, MEP recruitment curve, as well as cortical excitability measures (inhibition, facilitation).

Although the TMS has established itself as a useful tool in adult population, its great potential use in child population has yet to show.[10,11] So far, TMS is an established procedure in children to investigate the integrity and maturation of the motor system (corticospinal tract).[12–14] There is also a general consensus regarding the need of posing certain safety guidelines for TMS use in children,[10,11,15,16] since the child brain is considered to be significantly more plastic than the adult brain, resulting in longer lasting neuroplastic changes.[10]

Compared to adults, children under 10 years of age have higher motor-evoked potential thresholds (RMTs),[17] and children of 13.5 years of age have lower intracortical inhibition.[18] With the increasing age, RMT level declines until reaching the adult levels at 13–16 years,[19] while lower intracortical inhibition in children points to maturation process that may have implications for greater capacity of practice-dependent neuronal plasticity in children.[20] Nowadays, it is assumed that age-related differences in TMS-evoked parameters in children reflect primarily changes during the cerebral and corticospinal myelination, intracortical synaptic and neuronal developmental process.[11,15] Due to higher mean values and general variability between individuals, it has been suggested that determining RMTs may be less useful in children younger than 10 years.[19]

In addition to aforementioned stimulation settings that can be more or less adjusted to suit the needs of the TMS investigator, and the obvious difference in brain size between adult and child, the biological tissue parameters such as permittivity and the electrical conductivity will significantly affect the distribution of the induced fields in the brain. These dielectric tissue parameters are often very difficult to obtain, and in addition to being very inhomogeneous, they exhibit variations as well as 25% from their averages.[21] Several studies show the dielectric parameters of the brain tissue to have significant age-related variations,[22–24] primarily due to changes in tissue water content, and, moreover, the degree of these parameters uncertainty is even more pronounced at low frequencies. Furthermore, the effects of different TMS-stimulating protocols on cellular and molecular changes in neurons *in vitro* remain poorly understood.[25]

TMS modeling can be helpful in determining the exact location of stimulation in the interpretation of experimental results as well as designing more efficient stimulation setups. This modeling can also provide TMS investigator to get more reliable prediction of the induced fields and currents.

Some recent numerical studies showed the major influence of the electrical conductivity uncertainty on the induced electric field,[26] while others showed these effects to be

negligible,[27] and concluded rather that variations of the coil position and the brain size to have more effects on the induced electric fields.

The majority of a TMS computational methods use the so-called quasi-static approximation, where the capacitive effects and the effects of propagation are neglected. The crvena nTMS systems currently in clinical use also rely on this approximation as well as on the simple spherical conductor models to determine the induced electric field.[28] Although, the quasi-static approximation results in the simplification of the governing equations, the exclusion of propagation effects at very high values [29] of tissue permittivity [30] could lead to an incorrect assessment of the stimulated area.[31–33] A recent study using a DTI-based model showed that neglecting the permittivity values leads to a decrease in about 72% and 24% of the maximum currents and fields, respectively.[34] Hence, a rigorous, more accurate model, such as one reported in [35], could aid in finding out to what extent does the variation of brain tissue parameters influence the induced fields and currents. Also, it could be interesting to investigate the influence of the brain size, similar to electromagnetic-thermal dosimetric comparison in [36]. Also, as the analysis on animals [37] showed the reduced TMS-efficacy in smaller brain volumes, there is some concern on the use of adult size TMS coils in children.

To the best of our knowledge, only one previous analysis [38] has been carried out related to the variability of the TMS-induced fields in the adult and child brain models. However, the analysis in [38] did not take into account the capacitive effects neither the age-dependent parameters of the human brain. This paper is an extension of our preliminary work reported in [39]. It aims at elucidating some of the differences between the TMS-induced field distributions between adult and two scaled children's brain models based on the rigorous surface integral equation (SIE) framework while taking into account the age-related brain tissue parameters.

The paper is organized as follows: in the first part, the brief overview of a SIE-based model of a TMS is given. This part is followed by the description of the homogeneous adult brain model and the derivation of two smaller brain models of a 10-years and 5-years-old child. Finally, the numerical results are presented for the stimulation of three generic TMS coils as well as a discussion on the influence of various parameters on the induced fields and currents.

2. Methodology

2.1. Formulation

The problem of human brain exposed to TMS coil radiation is treated as a classical scattering problem. The electromagnetic field ($\vec{E}^{inc}, \vec{H}^{inc}$) is incident on the lossy homogeneous object representing the brain. Due to the presence of the scattering object, i.e. the brain, a scattered field denoted by ($\vec{E}^{sca}, \vec{H}^{sca}$) also exists.

To account for inductive and capacitive effects, the human brain is considered as a lossy material with complex permittivity and permeability (ϵ, μ), placed in free space. The value for the permeability of the brain is taken to be μ_0 , due to the fact that biological tissues do not possess magnetic properties. The complex permittivity of the brain is given by

$$\epsilon = \epsilon_0 \epsilon_r - j \frac{\sigma}{\omega} \quad (1)$$

where ε_0 is the permittivity of the free space, ε_r is the relative permittivity, σ is the electrical conductivity of the brain, and $\omega = 2\pi f$ is the operating frequency.

Using the equivalence theorem, two equivalent problems are formulated in terms of equivalent electric and magnetic current densities assumed to flow on the brain surface. [40,41] Applying the boundary conditions for the electric field at the surface S being the interface of the two equivalent problems

$$-\hat{n} \times \vec{E}_i^{sca}(\vec{J}, \vec{M}) = \begin{cases} \hat{n} \times \vec{E}^{inc}, & i = 1 \\ 0, & i = 2 \end{cases} \quad (2)$$

the electric field integral equation (EFIE) in the frequency domain for the lossy homogeneous human brain is obtained. In (2), \vec{E}^{inc} is the known incident field, generated by a TMS coil, while \vec{J} and \vec{M} represent unknown surface currents.

Under the assumption that TMS coil is decoupled from the human brain,[35] i.e. its presence does not disturb the field, the electric field due to the coil is given by

$$\vec{E} = -j\omega\vec{A} \quad (3)$$

Assuming the uniform current density I over a coil cross section, the magnetic vector potential at an arbitrary point can be obtained from the particular integral

$$\vec{A}(\vec{r}) = \frac{\mu_0 M I}{4\pi} \int_l \frac{d\vec{l}}{|\vec{r} - \vec{r}'|} \quad (4)$$

where μ_0 is the free space permeability, M is the number of coil windings, and $|\vec{r} - \vec{r}'|$ is the distance from the observation to the source point on the coil.

After taking some mathematical manipulations on (2), [35,42], the set of coupled integral equations is derived

$$j\omega\mu_i \int_S \vec{J}(\vec{r}') G_i(\vec{r}, \vec{r}') dS' - \frac{j}{\omega\varepsilon_i} \int_S \nabla_S' \cdot \vec{J}(\vec{r}') \nabla G_i(\vec{r}, \vec{r}') dS' + \int_S \vec{M}(\vec{r}') \times \nabla' G_i(\vec{r}, \vec{r}') dS' = \begin{cases} \vec{E}^{inc}, & i = 1 \\ 0, & i = 2. \end{cases} \quad (5)$$

The equivalent electric and magnetic currents \vec{J} and \vec{M} are expressed in terms of linear combination of RWG and $\hat{n} \times$ RWG basis functions, respectively.

Numerical solution of (5) is obtained via the Method of Moments (MoM) scheme leading to a matrix-type equation

$$[\mathbf{Z}]\{\mathbf{I}\} = \{\mathbf{V}\} \quad (6)$$

whose solution is a vector \mathbf{I} containing the unknown coefficients J_n and M_n , respectively. Calculating these coefficients, the equivalent currents \vec{J} and \vec{M} , and subsequently, the electric field and the magnetic field can be determined at an arbitrary point in brain, using

$$\begin{aligned}\vec{E}_2(\vec{r}) = & -j\omega\mu_2 \int_S \vec{J}(\vec{r}') G_2(\vec{r}, \vec{r}') dS' - \frac{j}{\omega\epsilon_2} \int_S \nabla'_S \cdot \vec{J}(\vec{r}') G_2(\vec{r}, \vec{r}') dS' \\ & - \int_S \vec{M}(\vec{r}') \times \nabla G_2(\vec{r}, \vec{r}') dS',\end{aligned}\quad (7)$$

and

$$\begin{aligned}\vec{H}_2(\vec{r}) = & -j\omega\epsilon_2 \int_S \vec{M}(\vec{r}') G_2(\vec{r}, \vec{r}') dS' - \frac{j}{\omega\mu_2} \int_S \nabla'_S \cdot \vec{M}(\vec{r}') G_2(\vec{r}, \vec{r}') dS' \\ & + \int_S \vec{J}(\vec{r}') \times \nabla' G_2(\vec{r}, \vec{r}') dS',\end{aligned}\quad (8)$$

respectively.

The magnetic flux density is

$$\vec{B} = \mu_0 \vec{H}. \quad (9)$$

where magnetic field \mathbf{H} is calculated using (8). The current density \vec{J}_{ind} induced in the lossy homogeneous brain is determined from

$$\vec{J}_{ind} = (\sigma + j\omega\epsilon_0\epsilon_r) \vec{E} \quad (10)$$

where σ and ϵ_r are the frequency-dependent electric conductivity and relative permittivity of the human brain, respectively.

2.2. Human brain models

It must be pointed out that the gyrification of the brain is important for the accurate determination of maximum induced electric field,[43,44] and therefore, it would be interesting to show any age-dependent changes in brain gyrification and their potential impact. The presented formulation can be used to this means, i.e. on a more detailed brain model, derived from the magnetic resonance images (MRI). But, due to difficulty in obtaining child brain MRI (due to ethical, in addition to technical reasons), as well as to facilitate the solution process, the smoothed brain surface model is featured in this work. We consider a brain compartment model only and neglect the skull and scalp because the majority of the current is flowing inside the skull.[45] Although the homogeneous brain model does not represent the realistic scenario, as the surrounding tissues will affect the distribution of the induced fields and currents,[46] the analysis in [47] showed that the inclusion of the skull or CSF would not affect the distribution of currents in the adjacent cortex. Also, study [48] showed that one compartment model, despite its simplicity, produces a quite robust results, and that it is almost as accurate as the three-layered model, thus offering a good balance between accuracy and the computational cost. Another study [49] presented similar trends of the electric field distribution along investigation line in the anatomical voxel model and the homogeneous head.

We assumed the average dimensions of the adult human brain to be: width 131.8 mm, length 161.1 mm, height 139 mm.[50] The models of 10-years-old (10-yo) and 5-years-old

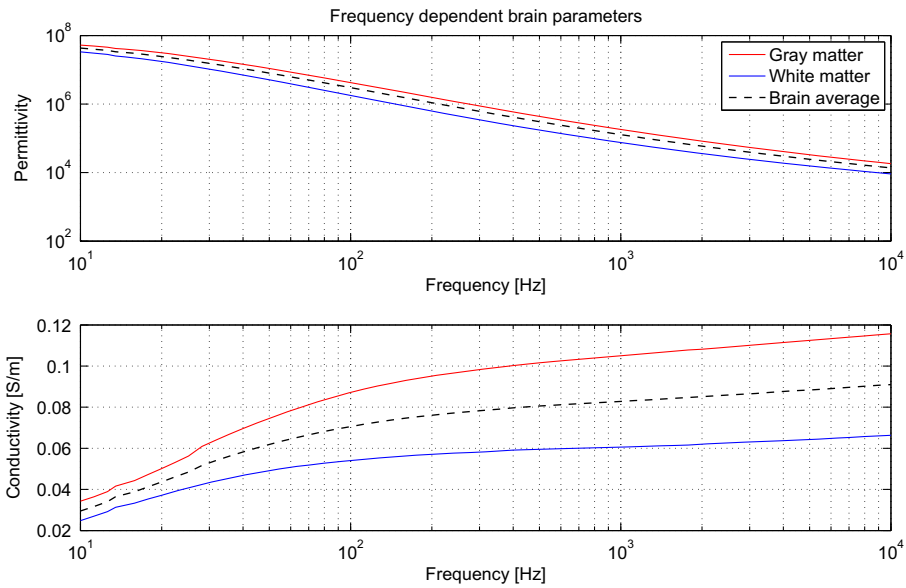


Figure 1. Frequency-dependent parameters of brain tissue, taken from [54].

(5-yo) child brain, respectively, are obtained by linearly scaling the model of an adult human brain, similar to the approach used in [51]. The applied scaling factors for the 10-yo and 5-yo brain are, 0.805 and 0.693 in the horizontal plane, while the vertical axis is scaled by 0.782 and 0.635, respectively.

It is worth noting that the child brain is not simply a scaled version of the adult brain, as the surrounding tissues such as skull and skin develop at different pace.[52] Nevertheless, this scaling approach can provide some insights into the sensitivity of the results due to variable brain dimensions. The assessment of the effects these and other uncertainties have on the resulting values of interest is currently the main challenge of stochastic dosimetry.[52] Although anatomically correct children models based on MRI data should be used when available, the majority of the studies using scaled models are consistent with anatomically correct models.[53]

2.3. Brain tissue parameters

It is often very hard to find the reliable values of the biological tissue parameters of interest. Moreover, these parameters vary significantly between healthy subjects and patients, as well as due to difference in age and sex. The significant effort has been put in [54] to acquire the reliable data on biological tissues and today represents the most frequently used reference for the non-living human and animal tissues. The brain tissue parameters such as permittivity and the electrical conductivity show the natural variation with frequency, as depicted in Figure 1.

The frequency-dependent parameters of the homogeneous adult human brain, given in Table 1, are taken from [54], as an average between the white matter and the gray matter.

The biological tissue parameters such as the permittivity and the electrical conductivity significantly affect the distribution of the induced fields in those tissues. The work on the rat

Table 1. The age-related parameters for the homogeneous human brain. The base (adult) parameters are taken from [54], as an average value of white and gray matter at particular frequency of interest. The parameters for two child models are scaled based on expressions from [58]. The scaling factors are given in the third and fifth rows.

Frequency (kHz)	Permittivity ϵ_r			Conductivity σ (S/m)		
	2.44	3	5	2.44	3	5
adult	46940	37290	24380	0.08595	0.0867	0.0884
10-years	58535	46135	29276	0.107	0.107	0.108
10-years/adult	1.2470	1.2372	1.2193	1.2249	1.2341	1.2217
5-years	72971	57062	36234	0.133	0.132	0.131
5-years/adult	1.5546	1.5302	1.4862	1.5474	1.5225	1.4819

brain [55] from the early 2000s reported the higher conductivity values in young rats, thus rekindling the questions whether the same is being true in human subjects as well. There are some measurements of the human brain tissue parameters [56] performed 10 hours post-mortem, but no reported studies on the changing values of parameters such as permittivity and conductivity in the living subjects.

Biological tissues contain a high proportion of water (TBW – Total Body Water content), which is reduced during the lifetime.[57] The most likely reason for tissue properties to change during the lifetime is water content, but so far there is still no sufficient studies to confirm this.[53] The fact that the dielectric properties of the tissues depend on this parameter has led to expressions that can evaluate the permittivity and conductivity of biological tissues depending on age,[58] i.e. on TBW content.

According to [58], the following expression can be used to derive the complex permittivity of a 10-years and a 5-years-old brain:

$$\epsilon = \epsilon_{rW}^{\frac{\alpha - \alpha_A}{1 - \alpha_A}} \epsilon_{rA}^{\frac{1 - \alpha}{1 - \alpha_A}} \left(1 - j \frac{1}{\omega \tau} \right) \quad (11)$$

where ϵ_{rW} is the relative permittivity of water, ϵ_{rA} is the relative permittivity of adult tissue, while α_A and α are the tissue hydration rates of adult and child, respectively, given by $\alpha = \rho \cdot TBW$, where ρ is the tissue density. The proposed fitting function for TBW is given by [58]

$$TBW = 784 - 241e^{-\left(\frac{\ln(Age/55)}{6.9589}\right)^2} \quad (12)$$

More details can be found in [58].

The parameters used in our two child models, at the three particular frequencies of interest (2.44, 3, and 5 kHz), are given in Table 1.

3. Numerical results and discussion

The numerical results for three typical TMS stimulation coils (circular, figure-of-eight and butterfly) are presented in this section. All coils are discretized to 80 linear segments. The radius of circular coil is 4.5 cm, while the radius of the 8-coil and the butterfly coil (10 degrees between wings) is 3.5 cm. The number of wire turns is 14 and 15, respectively, in

Table 2. Generic stimulating coil parameters. The coil current is of sinusoidal waveform (2.44, 3, 5 kHz).

	Circular coil	Figure-of-eight coil	Butterfly coil
Radius of turn	4.5 cm	3.5 cm	3.5 cm
Number of turns	14	15	15
Coil current	2.843 kA	2.843 kA	2.843 kA

circular coils and in other two coils. In all simulations, the coils and the surface of the brain (corresponding to primary motor cortex) were separated by 1 cm.

We choose to compare the three operating frequencies of the coils: 2.44 kHz, since the maximum of the induced current normalized amplitude occur at this frequency,[59] and two other frequencies most often used in the TMS analysis, 3 and 5 kHz, respectively. The amplitude of the current is 2.843 kA. Coil parameters are given in Table 2.

3.1. Adult brain parameters

The induced electric field, magnetic flux density, and the induced current density are calculated first using the adult tissue parameters in all three brain models, enabling the study of the brain size on the induced fields. Figure 2 illustrates the effects of brain size on the induced electric field distribution at the surface of three models, using three different coils at three frequencies.

Using the circular coil, the calculated maximum induced field is directly under the coil windings, while for the figure-of-eight and butterfly coils, it is concentrated over a small area under the coil's geometric center. In the smaller brain models, stimulation with the same size coil results in higher values of induced electric field dispersed over larger brain area (relative to the brain size). The higher values of maximum induced electric field are seen in smaller brain models, except for the circular coil. This could easily be attributed to the fact that in smaller brain models, the coil at the lateral brain parts is moved further from the surface, as seen in the first row in Figure 2.

For the other two coils, the maximum obtained values are at the brain surface directly under the coil center, while in brain parenchyma fields rapidly decay, as shown in Figure 3 for the figure-of-eight coil at $f = 3$ kHz. The maximum induced electric field value in two smaller models is higher than the value in the adult model, at the same time decreasing more rapidly, i.e. the field gradient is higher. Approximately 1.6 cm under the brain surface, the induced electric field values are similar for all three models.

Finally, the comparison of induced electric field in the adult brain model, due to stimulation by figure-of-eight coil at 2.44, 3, and 5 kHz, respectively, is given in Figure 4. The frequency-dependent parameters of the adult brain, given in Table 1, are used. Stimulation by a higher frequency (sinusoidal current waveform of the stimulation coil) results in higher values of the induced electric field. Dashed line denotes the depth from the brain surface at which the electric field falls to half its maximum value. At all three frequencies, the E_{\max} half value is obtained at the same depth.

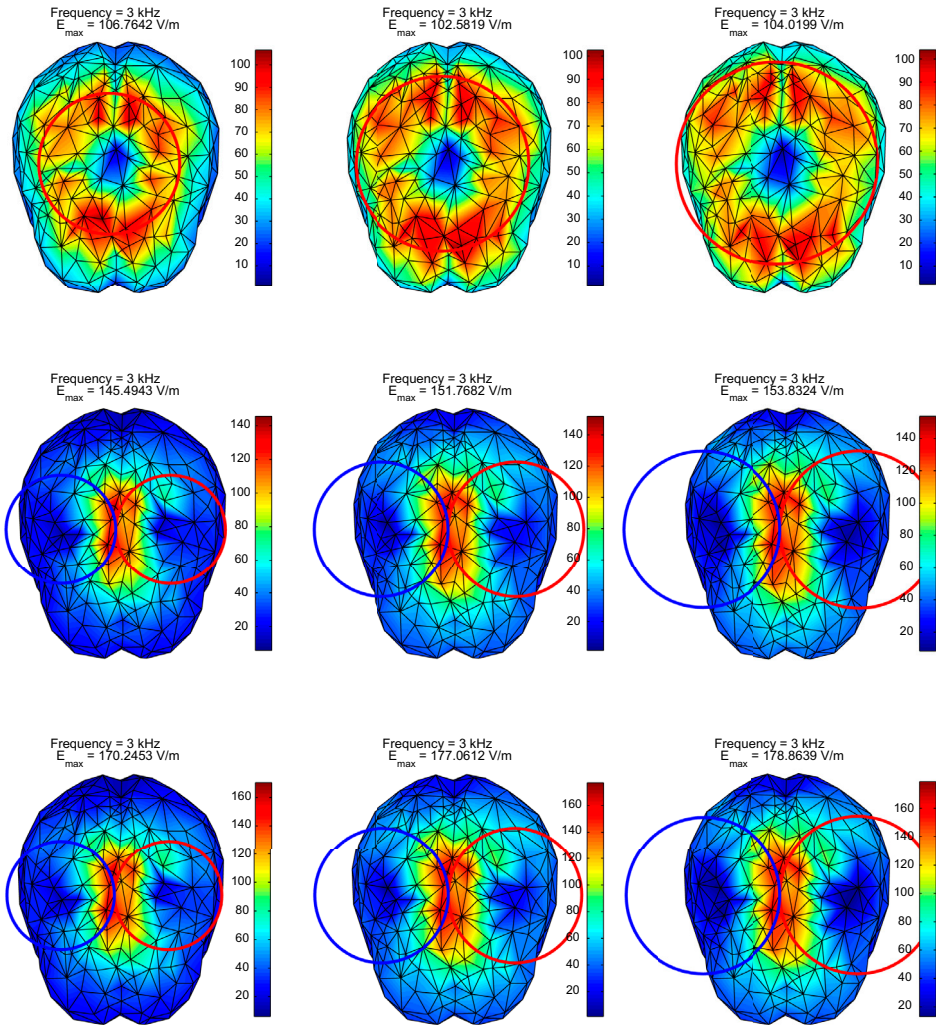


Figure 2. Induced electric field at the surface of adult, 10-years-old and 5-years-old brain models (left to right), stimulated with three different coils at 3 kHz (top to bottom). The adult brain parameters at this particular frequency are used in the child models.

3.2. Age-dependent parameters

Next, the results for the values of TMS-induced fields are obtained while taking into account the age-dependent tissue parameters for the two child models. Table 3 gives the results for the maximum values of induced electric field E_{max} , magnetic flux density B_{max} , and the induced current density J_{max} , respectively, in the adult and child models, stimulated by figure-of-eight coil at three frequencies. Inclusion of the age-dependent parameters (denoted by ϵ, σ subscript) in two smaller models, has the only effect on the increase in induced current density J_{max} , while E_{max} and B_{max} are practically the same. These results suggest that the adult brain parameters are sufficient when modeling homogeneous child brains and when interested in the induced electric field only (e.g. in finding a region where reaching an electric field threshold value will result in the activation

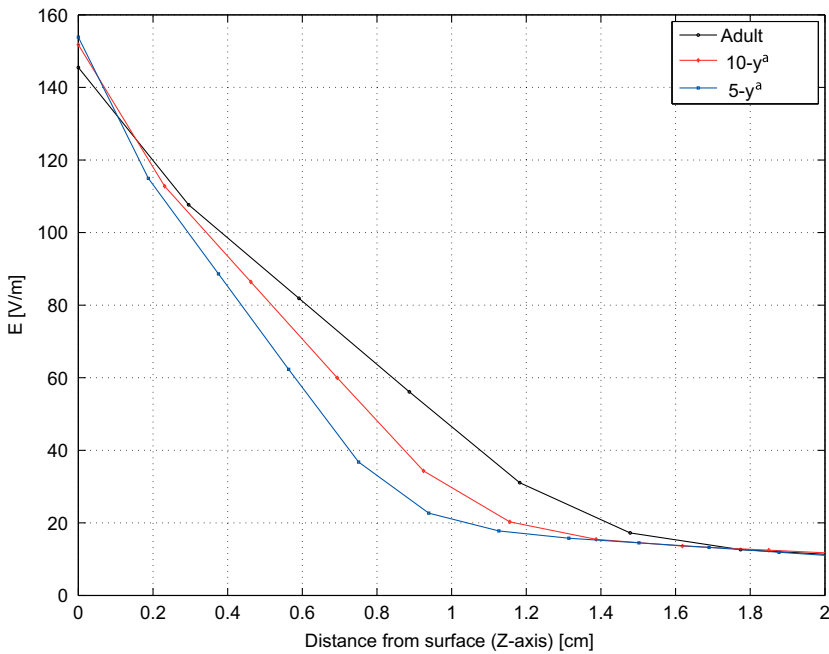


Figure 3. Comparison of induced electric field in the adult, 10-years-old, and 5-years-old brains stimulated by the figure-of-eight coil at 3 kHz. The adult brain parameters are used in the child models (denoted by subscript a). The location of points is directly under the geometric center of the coil.

Table 3. The maximum induced electric field E_{\max} , magnetic flux density B_{\max} , and the induced current density J_{\max} in the adult, 10-years-old, and 5-years-old brain models, respectively, stimulated by figure-of-eight coil at three frequencies (2.44, 3, 5 kHz).

	2.44 kHz			3 kHz			5 kHz		
	E_{\max} (V/m)	B_{\max} (T)	J_{\max} (A/m ²)	E_{\max} (V/m)	B_{\max} (T)	J_{\max} (A/m ²)	E_{\max} (V/m)	B_{\max} (T)	J_{\max} (A/m ²)
adult	118,280	0,6560	10,194	145,4943	0,6563	12,6468	242,4701	0,6556	21,4973
10-years ^a	123,378	0,7734	10,633	151,7682	0,7760	13,1922	252,8466	0,7749	22,4173
5-years ^a	125,122	0,8802	10,784	153,8282	0,8832	13,3712	256,3759	0,8831	22,7302
10-years $_{\epsilon, \sigma}$ ^b	123,370	0,7751	13,237	151,7821	0,7755	16,2827	252,8530	0,7748	27,3880
5-years $_{\epsilon, \sigma}$ ^b	125,090	0,8801	16,684	153,8256	0,8831	20,3578	256,3402	0,8827	33,6798

^aAdult tissue parameters used in child model.

^bAge dependent tissue parameters used in child model.

of that particular area). On the other hand, if one was interested into coupling the induced current and field distributions to neurophysiological equations,[60–62] i.e. for calculating the transmembrane potentials of the nerve fibers in the brain,[34] the age-dependent parameters should not be neglected.

Although the introduction of the age-dependent parameters in the child models did not have an effect on the maximum electric field value, it will have an effect on the electric field half maximum value distance from the surface, as seen in Figure 5. With smaller brain geometries, the point with $0.5E_{\max}$ is moved closer to the surface, i.e. for adult model this

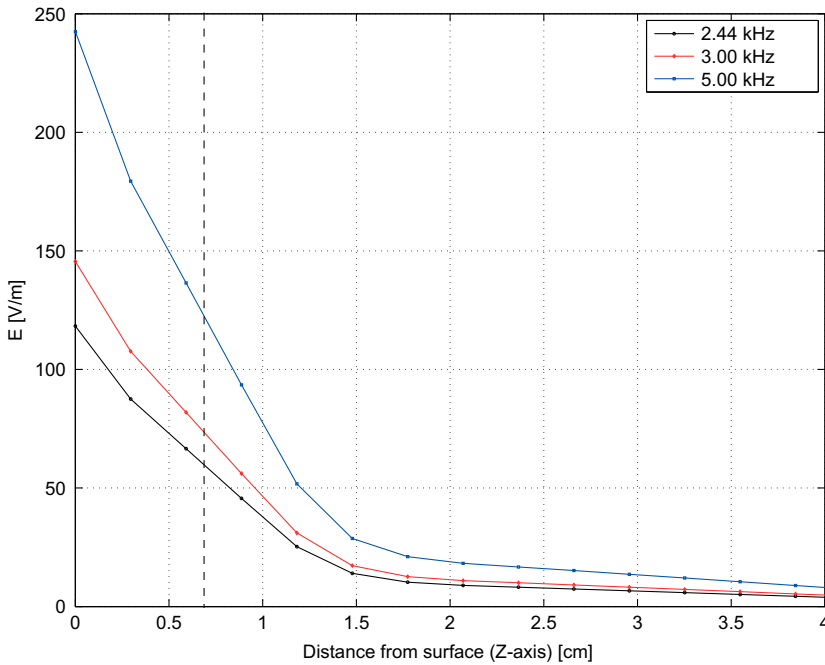


Figure 4. Comparison of induced electric field in the adult brain model, due to stimulation by figure-of-eight coil at 2.44, 3 and 5 kHz.

value is around 7 mm, while for 10-years-old and 5-years-old models, it is around 5.6 mm and 4.5 mm, respectively.

Figure 6 presents the cumulative effects of the brain size and the age-related parameters on the maximum induced current density J_{max} in three brain models using three different stimulation coils. Using the age-dependent brain parameters (solid lines), the decrease in brain size (age), is followed by the increase in the induced current values. Using adult parameters for the two child brain models (dashed lines), decrease in brain size is followed by a very small increase in the induced currents in all the cases except for the circular coils where induced currents are decreased. This can be attributed to the smaller brains, i.e. the induced currents will ‘spread’ over wider area under the coil windings (as shown on Figure 2), contrary to the figure-of-eight coil where the maximum values will be obtained in very narrow area under the coil geometric center.

Finally, the influence of single parameter (the relative permittivity and the conductivity of the brain, respectively) on the induced current density is given in Tables 4 and 5. The comparison of the induced current density values for the 10-years and 5-years-old models is given for the following tissue properties: (a) adult tissue parameters, (b) age-dependent parameters for both permittivity and the conductivity, (c) age-dependent parameter only for the permittivity, and (d) only for the conductivity. Results show that taking into account only the age dependence of the permittivity will have a very small effect on the induced current density, while the age dependence of the conductivity will have a major effect on the calculated current values. What is more interesting is that the induced current density is increased by the same factor used to scale the age-dependent parameters, as evident from Tables 1, 4 and 5.

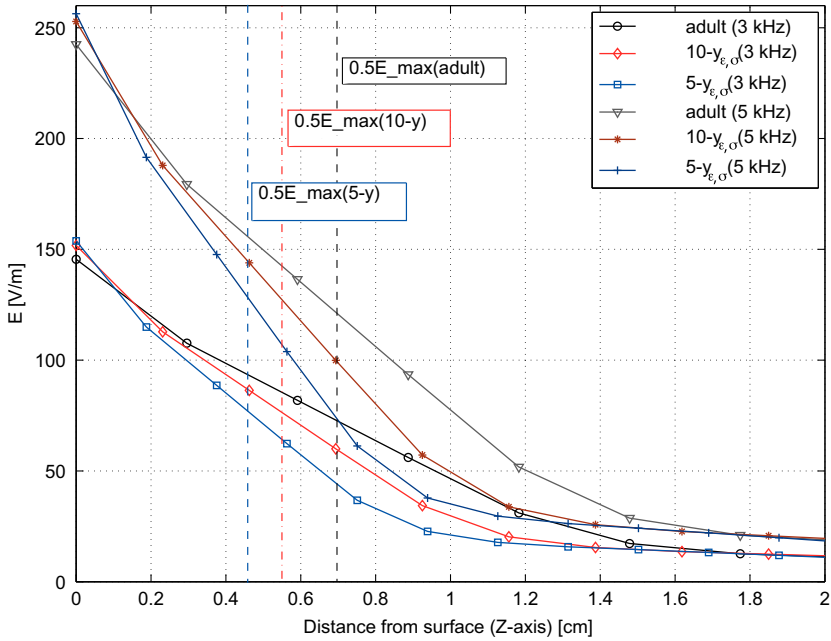


Figure 5. Comparison of induced electric field in the adult, 10-years-old, and 5-years-old brains stimulated by the figure-of-eight coil at 3 and 5 kHz. The age-related parameters are used in the child models (denoted by subscript ϵ, σ). Dashed vertical lines represent the distance from the brain surface where the maximum electric field value E_{max} (from the surface) falls to half its value. This distance is same for both frequencies.

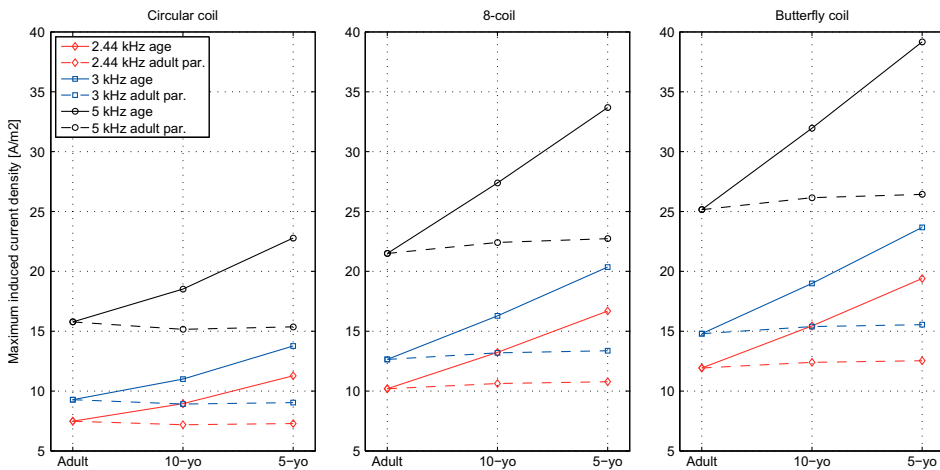


Figure 6. Comparison of a maximum induced current density J in three brain models using three different stimulation coils at 2.44, 3, and 5 kHz.

Table 4. The maximum induced current density J (A/m^2) in the 10-years-old brain model for three different coils at three frequencies.

Frequency (kHz)	Circular			8-coil			Butterfly		
	2.44	3	5	2.44	3	5	2.44	3	5
10-years ^a (A/m^2)	7.1901	8.9167	15.1577	10.633	13.1922	22.4173	12.404	15.3907	26.1537
10-years $\epsilon_r\sigma$ ^b (-)	1.2450	1.2336	1.2218	1.2449	1.2343	1.2217	1.2448	1.2342	1.2219
10-years ϵ ^c (-)	1.0015	1.0013	1.0015	1.0013	1.0011	1.0014	1.0012	1.0011	1.0014
10-years σ ^d (-)	1.2432	1.2331	1.2206	1.2433	1.2327	1.2206	1.2436	1.2327	1.2205

^aAdult tissue parameters used in child model.

^bAge-dependent tissue parameters used in child model. Induced currents normalized with respect to the values obtained using adult tissue parameters.

^cAge-dependent relative permittivity, adult parameters for conductivity.

^dAdult parameters for relative permittivity, age-dependent conductivity.

Table 5. The maximum induced current density J (A/m^2) in the 5-years-old brain model for three different coils at three frequencies.

Frequency (kHz)	Circular			8-coil			Butterfly		
	2.44	3	5	2.44	3	5	2.44	3	5
5-y ^a (A/m^2)	7.2911	9.0417	15.3703	10.7840	13.3712	22.7302	12.5380	15.5474	26.4312
5-y $\epsilon_r\sigma$ ^b (-)	1.5472	1.5222	1.4823	1.5471	1.5225	1.4817	1.5476	1.5225	1.4819
5-y ϵ ^c (-)	1.0045	1.0035	1.0038	1.0039	1.0035	1.0036	1.0039	1.0035	1.0034
5-y σ ^d (-)	1.5467	1.5203	1.4798	1.5448	1.5203	1.4769	1.5452	1.5204	1.4794

^aAdult tissue parameters used in child model.

^bAge-dependent tissue parameters used in child model. Induced currents normalized with respect to the values obtained using adult tissue parameters.

^cAge-dependent relative permittivity, adult parameters for conductivity.

^dAdult parameters for relative permittivity, age-dependent conductivity.

4. Conclusion

The work presented in this paper, based on the SIE formulation and related method of moments (MoM) solution is a part of an ongoing effort in developing a more accurate realistic model of the human brain, exposed to the field generated by TMS coils. In particular, numerical results for the electric field, current density and the magnetic flux density induced inside the adult, 10-years and 5-years-old child brain, respectively, are compared. The results obtained with two homogeneous child brain models showed the increased values of all TMS-induced fields, indicating the importance of using correct size when modeling the child brain. Although this work featured a simple scaling approach in obtaining brain models of children, it indicates that the detailed anatomical neuroimaging such as MRI is therefore essential for minimizing factors contributing to calculation variations. When modeling the TMS effects in the child brains, in addition to differences in the brain size, the age-related variation of tissue parameters should be taken into account, due to their critical influence on the induced intracerebral current density, particularly if one was interested in coupling the results with equations of neurophysiology. Elucidation of the differences of the cortical effects and TMS-induced fields in adult and child brain models may contribute to development of optimal TMS coils and stimulating parameters especially when applying TMS in diagnostic and rehabilitation of pediatric population with acquired brain injury.[63]

Disclosure statement

No potential conflict of interest was reported by the authors.

References

- [1] Barker AT, Jalinous R, Freeston IL. Non-invasive magnetic stimulation of the human motor cortex. *Lancet*. 1985;325:1106–1107.
- [2] Picht T, Krieg SM, Sollmann N, et al. A comparison of language mapping by preoperative navigated transcranial magnetic stimulation and direct cortical stimulation during awake surgery. *Neurosurgery*. 2013;72:808–819.
- [3] Rösler J, Niraula B, Strack V, et al. Language mapping in healthy volunteers and brain tumor patients with a novel navigated TMS system: evidence of tumor-induced plasticity. *Clin. Neurophysiology*. 2014;125:526–536.
- [4] Deletis V, Rogić M, Fernández-Conejero I, et al. Neurophysiologic markers in laryngeal muscles indicate functional anatomy of laryngeal primary motor cortex and premotor cortex in the caudal opercular part of inferior frontal gyrus. *Clin. Neurophysiology*. 2014;125:1912–1922.
- [5] Rogić M, Deletis V, Fernández-Conejero I. Inducing transient language disruptions by mapping of Broca's area with modified patterned repetitive transcranial magnetic stimulation protocol. *J. Neurosurgery*. 2014;120:1033–1041.
- [6] Rossini P, Barker A, Berardelli A, et al. Non-invasive electrical and magnetic stimulation of the brain, spinal cord and roots: basic principles and procedures for routine clinical application. report of an IFCN committee. *Electroencephalography Clin. Neurophysiology*. 1994;91:79–92.
- [7] Stokes MG, Chambers CD, Gould IC, et al. Simple metric for scaling motor threshold based on scalp-cortex distance: application to studies using transcranial magnetic stimulation. *J. Neurophysiology*. 2005;94:4520–4527.
- [8] Knecht S, Sommer J, Deppe M, et al. Scalp position and efficacy of transcranial magnetic stimulation. *Clin. Neurophysiology*. 2005;116:1988–1993.
- [9] Rossini P, Burke D, Chen R, et al. Non-invasive electrical and magnetic stimulation of the brain, spinal cord, roots and peripheral nerves: basic principles and procedures for routine clinical and research application. An updated report from an IFCN Committee. *Clin. Neurophysiology*. 2015;126:1071–1107.
- [10] Frye RE, Rotenberg A, Ousley M, et al. Transcranial magnetic stimulation in child neurology: current and future directions. *J. Child Neurology*. 2008;23:79–96.
- [11] Rajapakse T, Kirton A. Non-invasive brain stimulation in children: applications and future directions. *Translational Neurosci*. 2013;4:1–29.
- [12] Müller K, Hömberg V. Development of speed of repetitive movements in children is determined by structural changes in corticospinal efferents. *Neurosci. Lett*. 1992;144:57–60.
- [13] Müller K, Hömberg V, Aulich A, et al. Magneto-electrical stimulation of motor cortex in children with motor disturbances. *Electroencephalography Clin. Neurophysiology/Evoked Potentials Section*. 1992;85:86–94.
- [14] Eyre J, Miller S, Clowry G, et al. Functional corticospinal projections are established prenatally in the human foetus permitting involvement in the development of spinal motor centres. *Brain*. 2000;123:51–64.
- [15] Garvey MA, Mall V. Transcranial magnetic stimulation in children. *Clin. Neurophysiology*. 2008;119:973–984.
- [16] Krishnan C, Santos L, Peterson MD, et al. Safety of noninvasive brain stimulation in children and adolescents. *Brain Stimulation*. 2015;8:76–87.
- [17] Garvey MA, Gilbert DL. Transcranial magnetic stimulation in children. *Eur. J. Paediatric Neurology*. 2004;8:7–19.
- [18] Mall V, Berweck S, Fietzek U, et al. Low level of intracortical inhibition in children shown by transcranial magnetic stimulation. *Neuropediatrics*. 2004;35:120–125.
- [19] Lin K, Pascual-Leone A. Transcranial magnetic stimulation and its applications in children. *Chang Gung Med. J*. 2002;25:424–436.

- [20] Ziemann U, Muellbacher W, Hallett M, et al. Modulation of practice-dependent plasticity in human motor cortex. *Brain*. **2001**;124:1171–1181.
- [21] Gabriel S, Lau R, Gabriel C. The dielectric properties of biological tissues: II. Measurements in the frequency range 10 Hz to 20 GHz. *Phys. Med. Biol.* **1996**;41:2251–2269.
- [22] Schmid G, Überbacher R. Age dependence of dielectric properties of bovine brain and ocular tissues in the frequency range of 400 MHz to 18 GHz. *Phys. Med. Biol.* **2005**;50:4711–4720.
- [23] Peyman A, Holden S, Watts S, et al. Dielectric properties of porcine cerebrospinal tissues at microwave frequencies: in vivo, in vitro and systematic variation with age. *Phys. Med. Biol.* **2007**;52:2229–2245.
- [24] Peyman A, Gabriel C, Grant E, et al. Variation of the dielectric properties of tissues with age: the effect on the values of sar in children when exposed to walkie-talkie devices. *Phys. Med. Biol.* **2008**;54:227–241.
- [25] Grehl S, Viola HM, Fuller-Carter PI, et al. Cellular and molecular changes to cortical neurons following low intensity repetitive magnetic stimulation at different frequencies. *Brain Stimulation*. **2015**;8:114–123.
- [26] Weise K, Di Rienzo L, Brauer H, et al. Uncertainty analysis in transcranial magnetic stimulation using noninvasive polynomial chaos expansion. *IEEE Trans. Magn.* **2015**;51:1–8.
- [27] Gomez L, Yucel A, Hernandez-Garcia L, et al. Uncertainty quantification in transcranial magnetic stimulation via high-dimensional model representation. *IEEE Trans. Biomed. Eng.* **2015**;62:361–372.
- [28] Ruohonen J, Karhu J. Navigated transcranial magnetic stimulation. *Neurophysiologie Clinique/Clin. Neurophysiology*. **2010**;40:7–17.
- [29] Wagner T, Zahn M, Grodzinsky A, et al. Three-dimensional head model simulation of transcranial magnetic stimulation. *IEEE Trans. Biomed. Eng.* **2004**;51:1586–1598.
- [30] Stoykov NS, Lowery MM, Taflove A, et al. Frequency- and time-domain FEM models of EMG: capacitive effects and aspects of dispersion. *IEEE Trans. Biomed. Eng.* **2002**;49:763–772.
- [31] Butson C, McIntyre C. Tissue and electrode capacitance reduce neural activation volumes during deep brain stimulation. *Clin. Neurophysiology*. **2005**;116:2490–2500.
- [32] Tracey B, Williams M. Computationally efficient bioelectric field modeling and effects of frequency-dependent tissue capacitance. *J. Neural Eng.* **2011**;8:1–7.
- [33] Bossetti CA, Birdno MJ, Grill WM. Analysis of the quasi-static approximation for calculating potentials generated by neural stimulation. *J. Neural Eng.* **2008**;5:44–53.
- [34] De Geeter N, Crevecoeur G, Dupré L, et al. A DTI-based model for TMS using the independent impedance method with frequency-dependent tissue parameters. *Phys. Med. Biol.* **2012**;57:2169–2188.
- [35] Cvetković M, Poljak D, Haueisen J. Analysis of transcranial magnetic stimulation based on the surface integral equation formulation. *IEEE Trans. Biomed. Eng.* **2015**;62:1535–1545.
- [36] Cvetković M, Poljak D. Electromagnetic-thermal dosimetry comparison of the homogeneous adult and child brain models based on the SIE approach. *J. Electromagnet. Waves Appl.* **2015**;29:2365–2379.
- [37] Weissman JD, Epstein CM, Davey KR. Magnetic brain stimulation and brain size: relevance to animal studies. *Electroencephalography Clin. Neurophysiology*. **1992**;85:215–219.
- [38] Lu M, Ueno S. A comparison of induced electric fields in child and adult head models by transcranial magnetic stimulation; General Assembly and Scientific Symposium, 2011; XXXth URSI. Istanbul, Turkey; 2011 Aug; p. 1–4.
- [39] Cvetkovic M, Poljak D. Comparison of a TMS induced fields in homogeneous adult and child brain models using the surface integral equation approach; In: International Conference on Electromagnetics in Advanced Applications (ICEAA); 2015 Sep; Torino, Italy: IEEE; **2015**, p. 199–202.
- [40] Harrington R. Boundary integral formulations for homogeneous material bodies. *J. Electromagnet. Waves Appl.* **1989**;3:1–15.
- [41] Poggio AJ, Miller EK. Integral equation solutions of three-dimensional scattering problems. In: Mittra R, editor. *Computer techniques for electromagnetics*. 2nd ed. Chapter 4; Washington (DC): Hemisphere; **1987**. p. 159–264.

- [42] Cvetković M, Poljak D. An efficient integral equation based dosimetry model of the human brain. In: Proceedings of 2014 International Symposium on Electromagnetic Compatibility (EMC EUROPE); 2014 Sep 1–4; Gothenburg, Sweden; p. 375–380.
- [43] Chen M, Mogul DJ. Using increased structural detail of the cortex to improve the accuracy of modeling the effects of transcranial magnetic stimulation on neocortical activation. *IEEE Trans. Biomed. Eng.* **2010**;57:1216–1226.
- [44] Opitz A, Windhoff M, Heidemann RM, et al. How the brain tissue shapes the electric field induced by transcranial magnetic stimulation. *Neuroimage.* **2011**;58:849–859.
- [45] Stenroos M, Hunold A, Hauelsen J. Comparison of three-shell and simplified volume conductor models in magnetoencephalography. *NeuroImage.* **2014**;1–12. doi:10.1016/j.neuroimage.2014.01.006
- [46] Miranda PC, Hallett M, Basser PJ. The electric field induced in the brain by magnetic stimulation: a 3-D finite-element analysis of the effect of tissue heterogeneity and anisotropy. *IEEE Trans. Biomed. Eng.* **2003**;50:1074–1085.
- [47] Golestanirad L, Mattes M, Mosig J, et al. Effect of model accuracy on the result of computed current densities in the simulation of transcranial magnetic stimulation. *IEEE Trans. Magn.* **2010**;46:4046–4051.
- [48] Nummenmaa A, Stenroos M, Ilmoniemi RJ, et al. Comparison of spherical and realistically shaped boundary element head models for transcranial magnetic stimulation navigation. *Clin. Neurophysiology.* **2013**;124:1995–2007. doi:10.1016/j.clinph.2013.04.019
- [49] Bottauscio O, Chiampi M, Zilberti L, et al. Evaluation of electromagnetic phenomena induced by transcranial magnetic stimulation. *IEEE Trans. Magn.* **2014**;50:1033–1036.
- [50] Blinkov SM, Glezer II. The human brain in figures and tables. A quantitative handbook. New York (NY): Plenum Press; **1968**.
- [51] Bit-Babik G, Guy AW, Chou CK, et al. Simulation of exposure and SAR estimation for adult and child heads exposed to radiofrequency energy from portable communication devices. *Radiat. Res.* **2005**;163:580–590.
- [52] Wiart J, Hadjem A, Wong MF, et al. Analysis of RF exposure in the head tissues of children and adults. *Phys. Med. Biol.* **2008**;53:3681–3695.
- [53] Christ A, Kuster N. Differences in RF energy absorption in the heads of adults and children. *Bioelectromagnetics.* **2005**;26:31–44.
- [54] Gabriel C. Compilation of the dielectric properties of body tissues at RF and microwave frequencies. Brooks Air Force Base, TX. Report: AL/OE-TR-1996-0037; **1996**.
- [55] Peyman A, Rezazadeh AA, Gabriel C. Changes in the dielectric properties of rat tissue as a function of age at microwave frequencies. *Phys. Med. Biol.* **2001**;46:1617–1629.
- [56] Schmid G, Neubauer G, Mazal PR. Dielectric properties of human brain tissue measured less than 10 h postmortem at frequencies from 800 to 2450 MHz. *Bioelectromagnetics.* **2003**;24:423–430.
- [57] Shock N, Watkin D, Yiengst M, et al. Age differences in the water content of the body as related to basal oxygen consumption in males. *J. Gerontology.* **1963**;18:1–8.
- [58] Wang J, Fujiwara O, Watanabe S. Approximation of aging effect on dielectric tissue properties for SAR assessment of mobile telephones. *IEEE Trans. Electromagnet. Compat.* **2006**;48:408–413.
- [59] Kowalski T, Silny J, Buchner H. Current density threshold for the stimulation of neurons in the motor cortex area. *Bioelectromagnetics.* **2002**;23:421–428.
- [60] Hodgkin AL, Huxley AF. A quantitative description of membrane current and its application to conduction and excitation in nerve. *J. Phys.* **1952**;117:500–544.
- [61] Roth BJ, Basser PJ. A model of the stimulation of a nerve fiber by electromagnetic induction. *IEEE Trans. Biomed. Eng.* **1990**;37:588–597.
- [62] Rattay F. The basic mechanism for the electrical stimulation of the nervous system. *Neuroscience.* **1999**;89:335–346.
- [63] Chung MG, Lo WD. Noninvasive brain stimulation: the potential for use in the rehabilitation of pediatric acquired brain injury. *Arch. Phys. Med. Rehabil.* **2015**;96:S129–S137.